applied sciences

Article

Analysis of Bluetooth RSSI for Proximity Detection of Ship Passengers

Qianfeng Lin [1] and Jooyoung Son [2,*]

[1] Department of Computer Engineering, Korea Maritime and Ocean University, Busan 49112, Korea; linqianfeng@g.kmou.ac.kr
[2] Division of Marine IT Engineering, Korea Maritime and Ocean University, Busan 49112, Korea
* Correspondence: mmlab@kmou.ac.kr

Featured Application: This paper carries out an analysis on Bluetooth RSSI data according to different poses. The related analysis results can provide a reference basis for research on proximity detection algorithms for ship passengers.

Abstract: Concern about the health of people who traveled onboard was raised during the COVID-19 outbreak on the Diamond Princess cruise ship. The ship's narrow space offers an environment conducive to the virus's spread. Close contact isolation remains one of the most critical current measures to stop the virus's rapid spread. Contacts can be identified efficiently by detecting intelligent devices nearby. The smartphone's Bluetooth RSSI signal is essential data for proximity detection. This paper analyzes Bluetooth RSSI signals available to the public and compares RSSI signals in two distinct poses: standing and sitting. These features can improve accuracy and provide an essential basis for creating algorithms for proximity detection. This allows for improved accuracy in identifying close contacts and can help ships sustainably manage persons onboard in the post-epidemic era.

Keywords: COVID-19; received signal strength indicator; proximity detection; ship passenger

check for updates

Citation: Lin, Q.; Son, J. Analysis of Bluetooth RSSI for Proximity Detection of Ship Passengers. *Appl. Sci.* **2022**, *12*, 517. https://doi.org/10.3390/app12010517

Received: 8 November 2021
Accepted: 30 December 2021
Published: 5 January 2022

1. Introduction

Cruise ships have contributed to the spread of COVID-19 worldwide [1]. The Japanese government ordered passengers and crew on the Diamond Princess to start a two-week quarantine after a former passenger tested positive for COVID-19 [2]. Shipboard personnel remain at high risk for an infectious disease outbreak from COVID-19. A rapid and coordinated response is essential to containing the spread of Severe Acute Respiratory Syndrome Coronavirus 2 (SARS-CoV-2) [3]. The importation of viruses onboard is facilitated by regular and irregular contact with land-based populations. Living in confined spaces with limited air exchange promotes the spread of disease [4,5] and highlights the high risk of SARS-CoV-2 transmission on cruise ships. Close-range contact and communications likely contributed similarly to disease progression aboard the ship [6]. Crew members are one of the occupational groups more susceptible to outbreaks of this virus due to the cramped working environment [7].

Infectious diseases are more prone to spread quickly in this setting due to ships' restricted and limited interiors. Isolation is still one of the most effective ways to keep COVID-19 from spreading rapidly today. Those with confirmed COVID-19 and close contacts are the two main groups of people who will need to be quarantined. Finding and isolating close contacts is critical to halting COVID-19 rapid spread. Using smartphone location data to track close contacts is an excellent approach to finding them. Based on mobile sensor data from Smart Contact Tracking, 627,386 potential contacts related to Diamond Princess cruise ship passengers were identified by using location methods and analysis after cross validation with other sensor monitoring data [8]. Reference [8] also uses mobile sensor data to track close contacts. Bluetooth RSSI is precisely one of the mobile sensor data. The idea of our paper is to use Bluetooth RSSI from smartphones for proximity detection for close contact tracking. Using location information to track close contacts is not the only method. This can also be accomplished by adjusting device distances between cellphones. This technology separation is also known as proximity detection.

When faced with the threat of COVID-19, a highly contagious virus, maintaining proximity detection is an effective method to prevent infection. Specifically, the risk of COVID-19 transmission increases when an uninfected person is less than 6 ft away for more than 15 min from an infected person (also known as "too close for too long" (TCTL)). If a list of TCTL people could be detected and passively tracked via smartphones, users could be notified if they test positive for COVID-19. Existing radio frequency (RF) location technologies could be used to track the daily movements of infected smartphone users. Owners of neighboring smart devices can then be notified to maintain proximity detection or be tested if they are exposed to infected people.

Ubiquitous Bluetooth Low Energy (BLE) attracted significant attention due to its short-range and low energy consumption. The Massachusetts Institute of Technology (MIT) leads the Private Automated Contact Tracing (PACT) consortium [9]. The consortium provides several high-quality BLE Received Signal Strength Indicator (RSSI) datasets [9]. These data are collected in various proximity scenarios. The reliability analysis of RSSI-based BLE ranging is a complex issue. Practical measurement studies and characterization of proximity detection using BLE RSSI have been carried out in various scenarios [10]. Several previous studies have proposed methods to improve RSSI-based proximity detection. In addition to proximity, other researchers have used RSSI to estimate mutual orientation between users [11] and energy consumption of BLE RSSI proximity detection [12].

In most cases, Bluetooth RSSI is used in indoor positioning technology. In comparison to room size, the most critical components impacting RSSI during the development of indoor positioning algorithms are walls, metal materials, and water. The transmitter emits signals to the surrounding environment, although the signs are generally reflected due to walls and metal elements. As a result, misleading signals are generated. Human mobility is required in typical interior placement settings, and the human body is primarily made of water, which has a significant impact on RSSI signals. The preceding describes a typical internal placement scenario. Proximity detection, on the other hand, is not the same as traditional interior positioning scenarios. The transmitter and receiver in a proximity detection application are commonly two cellphones. The transmitter is frequently on a wall in classic indoor localization methods. A significant distance often separates the transmitter and receiver in proximity detection. The focus of proximity detection is on proximity. Two smartphone devices are pretty close to one other in practice. Proximity detection aims to discriminate between distant and near situations, not compute distance. Significantly, unlike previous proximity detection approaches, the proximity detection discussed in this study does not add closeness via sensing distance but instead directly uses RSSI. After distance is no longer a factor, the scenarios for proximity sensing are relatively similar, whether in a ship or a typical interior setting. As a result, the relevant conclusions gained through the dataset utilized in this study also apply to the ship environment.

RSSI can be considered as sensor data referring to indoor locations. However, the characteristics of RSSI such as Bluetooth have been rarely studied. This is true despite the vast knowledge about RF phenomena and received signal properties in indoor environments. Since RSSI is not intended to be used as a position sensor, there may be inherent performance limitations in using RSSI to determine position. Its statistical distribution is expected to differ from other indoor radio propagation studies that use sophisticated equipment such as vector signal analyzers to collect received signal data. The main objective of this study is to understand the various properties of RSSI associated with proximity detection through statistical data analysis of RSSI.

It is important to perform basic mathematical statistics on RSSI in this study. The apparent outcome is attained, and the results are declared by common sense. Our paper does not only obtain this result alone but also other exciting developments.

Our paper analyzes Bluetooth RSSI signals available to the public and compares RSSI signals in two distinct poses: standing and sitting. These features can improve accuracy and provide an essential basis for creating algorithms for proximity detection. This enhances accurate identification of close contacts and enables COVID-19 to be stopped further within a ship.

2. Related Works

Many studies on indoor positioning systems have pointed out the properties of the RSSI describing location fingerprints. In the seminal work of [13], the user's orientation may result in variations in RSSI levels of up to 5 dBm. However, no analysis of RSSI data is provided. Different directions of the user and mobile device concerning the access point may change the average value of RSSI at a location. The authors of [14] also suggest that the orientation should be included in calculating the user's location. The authors of [15] studied indoor positioning systems and considered user orientation by adding a digital compass to the mobile device to improve positioning accuracy. However, the increase from two to eight directions does not significantly improve localization performance. A preliminary study on the use of RSSI for location fingerprinting is reported in [16]. The researcher performs several RSSI measurements influenced by the user, orientation, and fade. The researcher finds that mean RSSI values changed, but RSSI values fluctuated more. This finding emphasizes the need to consider the influence of the user. Since RSSI can be used to calculate distance, it became the primary method for proximity detection, but user behavior significantly impacts RSSI. In other words, the user's pose fluctuates and affects RSSI signal. It is necessary to determine the impact that different user poses will have on the RSSI, which plays a crucial role in improving proximity detection accuracy. Proximity detection can be achieved by indoor positioning techniques, although it can also be reached directly by RSSI values. Applying machine learning algorithms to achieve RSSI proximity detection is a classification problem. The authors of [17] focused on using RSSI data to identify whether two persons are 6 ft apart by using machine learning classification techniques. The authors of [18] studied, using a machine learning approach, making inferences from the data collected by the sensor array to observe whether obtaining classifiers and a regressor on the projected distance between objects and the sensor is possible. The author of [19] uses classical estimation theory and several machine learning techniques to compare the accuracy of proximity distances and accompanying confidence levels. The author of [19] demonstrates that machine learning techniques may improve accuracy from 3.60 to 19.98 percent, bringing them closer to the feasible estimate bound. Therefore, this article uses distance to represent proximity. However, what our paper proposes is that there is a relationship between RSSI intensity and proximity, and proximity is not defined by distance but by RSSI power. This is the most fundamental difference between our paper and this article.

However, most of the studies in the literature do not further investigate the actual statistical properties of RSSI samples. Most of the existing studies on indoor localization focus on algorithms but do not analyze RSSI data. Therefore, in this study, we analyze RSSI data statistically from people's sitting and standing poses in order to analyze what kind of influence different poses have on RSSI and to consider this influence for proximity detection in the future to obtain accurate proximity detection. We first describe the MITRE range angle structured (MRAS) PACT dataset. Next, RSSI values are statistically analyzed in order to compare differences in mean, median, mode, standard deviation, and skewness at different distances and compare different poses. In addition, the differences in RSSI distributions at different poses are compared at exact distances.

This paper's main contribution is that using the mean value of RSSI brings more minor proximity detection errors than by using the median, mode, minimum, and maximum. If only RSSI dispersion is considered, it is difficult to reduce the error. Moreover, in most cases, RSSI values almost belong to the left-skewed distribution. There is a combination of mean and skewness of RSSI at different poses. In the case of close distances, the current posture of the person onboard can be identified based on the mean and skewness of RSSI. As distance increases, the difference in RSSI in various poses decreases. The mean and skewness features for distinguishing different poses will gradually disappear. In the case of close distance, the RSSIs of different poses have various fluctuation intervals in different periods. These features can improve the accuracy of proximity detection and identify the pose of ship passengers under certain conditions. Under the condition of proximity detection with high precision, close contacts can be accurately determined, thus preventing COVID-19 from spreading further inside the ship.

3. The PACT Proximity Datasets

The Too Close for Too Long (TC4TL) challenge, organized by the National Institute of Standards and Technology (NIST) in collaboration with the MIT PACT project, aims to improve proximity detection for Bluetooth Low Energy (BLE)-based contact tracking.

The PACT consortium published seven datasets. MRAS dataset is well documented in other datasets. Moreover, it contains measurements at different distances relevant to our study goals of performance evaluation of COVID-19 proximity detection from BLE RSSI measurements. The MRAS dataset also contains different tester pose settings. Environment settings specify the properties of the testing area, such as the room size and the tester's location in the room. Tester settings define how testers use devices and how they hold smartphones in addition to testers' poses. Testers pose either by "sitting" or "standing" at the marked location. Figure 1 shows BLE RSSI measurement scenarios for short-range operations of up to 15 ft. Eight stationary locations for measurement begin at 3 ft, are increased at intervals and end at 15 ft. The distances are identified relative to a person who holds a smartphone with BLE beacons. RSSI measurement data are collected by another person (a receiver) positioned at the eight labeled distances.

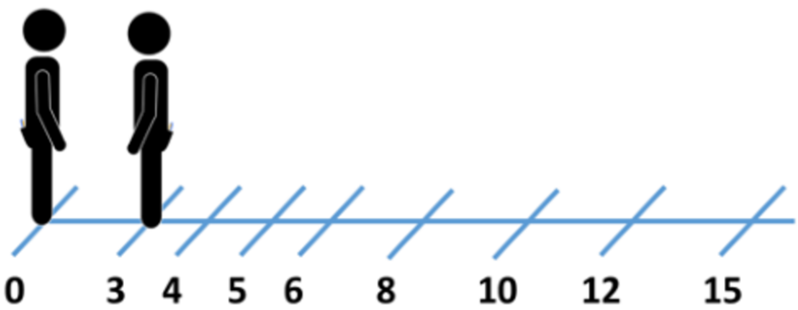

Figure 1. Eight distances for measurements of the RSSI database (source: PACT website).

These datasets are collected by using three versions of the Range-Angle Collection Protocol [20]: Short, Mid, and Full. The Full protocol consists of 40 datasets with RSSI measurements at eight different distances, as shown in Figure 1, and this study uses these datasets for performance evaluation for various distances. This study did not include Short and Mid versions, which had only two different distances of 3 ft and 8 ft and did not offer adequate diversity in measurement distances.

HANNARA is a Korean Maritime and Ocean University student training ship. Figure 2 depicts the layout of the HANNARA ship's student living quarters. The purpose of showing a plan of the HANNARA is that the ship environment is similar to that of a cruise ship, and there are enough persons on board as well. In addition, the ship has many stateroom structures similar to those on a cruise ship. It is possible to demonstrate the natural application environment of proximity detection to the maximum extent. The HANNARA ship is used as an experimental environment for this study in subsequent research. As shown in Figure 2, the vessel is compact, and proximity detections of less than 6 ft are more likely in this context. Due to the fact that ship space is restricted, the passengers onboard must engage in a full range of activities. Socialization distances of less than 6 ft and duration of more than 15 min are more frequent in this instance. As a result, one of the most critical aspects of locating close relationships is accurately calculating proximity detection of ship riders.

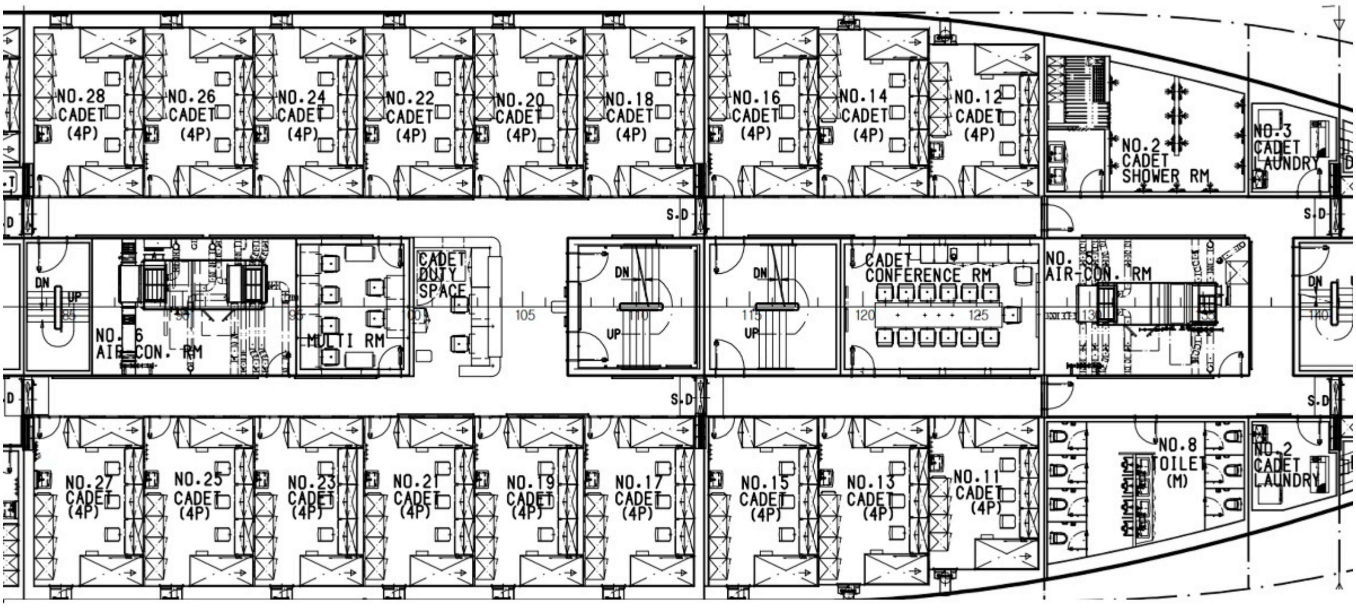

Figure 2. Floor plan of the HANNARA ship student housing quarters.

Figure 3 illustrates a practical application case of proximity detection. Firstly, the location information of the person riding the boat is obtained by an indoor positioning algorithm. It is assumed that the trajectory data of the COVID-19 confirmed person is known. The trajectories similar to COVID-19 are found by a clustering algorithm (DBSCAN (Density-based spatial clustering of applications with noise), as an example), and its user ID is obtained in order to classify it as a close contact. The results of proximity detection are combined at this time to finalize close contacts. Proximity detection can also confirm whether the close contacts are in the room. Let us suppose the door lock of a room has a Bluetooth signal transmitter. When the close contact leaves the room, proximity detection is suspended as RSSI strength changes dramatically and fades to nothing. Not obtaining proximity makes it possible to determine whether the close contact has left the isolated room without permission.

If the device proximity of a smartphone is known in addition to the COVID-19 patient and close contacts, then distance data can be tagged, and a machine learning method, such as the DBSCAN algorithm, is used to discover trends. The computer can find close contacts by learning the rules on its own, which will result in a significant increase in efficiency and accuracy. Close contacts are isolated according to epidemic prevention regulations after accurately identifying connections in a short period of time. An electronic barrier is set up in the isolation area of close contacts. Suppose a close contact leaves the isolation area without permission. In that case, a warning is sent to the monitoring room via a cell phone voice triggering device, and personnel can intervene in time to decrease the danger of viral transmission. As a result, distance recognition accuracy becomes highly critical.

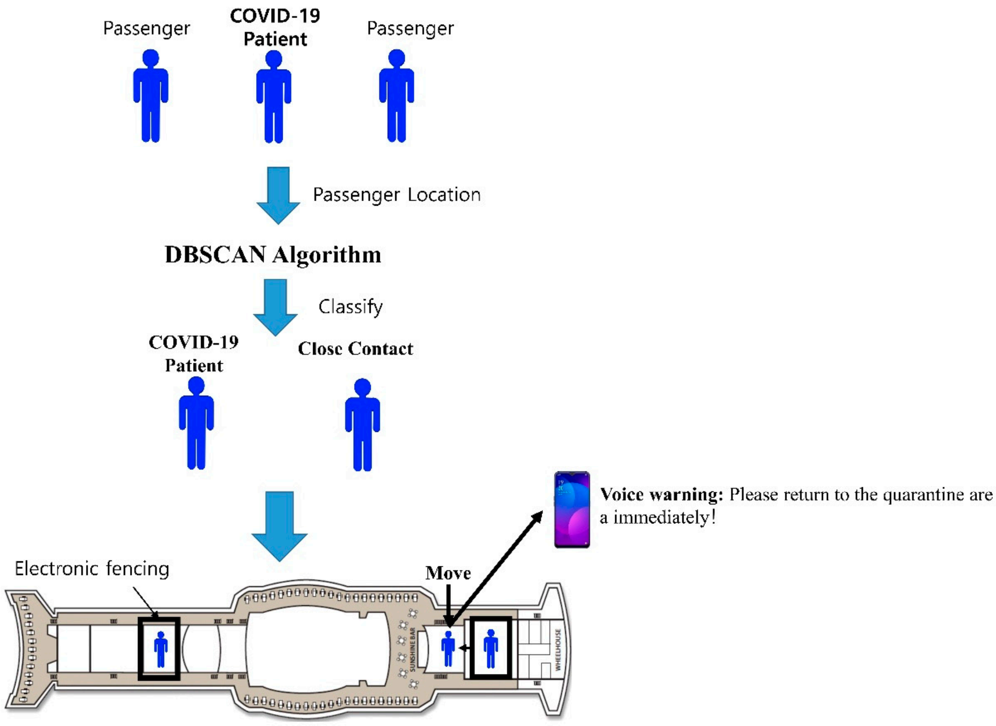

Figure 3. An illustration of how developing technologies can be used to find close contacts [21].

For proximity detection applications, the ship does not require additional equipment but only a smartphone in the hands of persons onboard. Generally, wireless networks are installed on newly built ships. The ship's wireless network covers the active area of the ship's occupants. RSSI data received from another person on the cell phone estimates proximity. Estimation results can be transmitted back to the control center by using WiFi. The server will store data in the local database to make it easier for the program to read the data. In older ships, a ship's wireless network has to be installed to be able to obtain proximity detection results from the user's device and to transmit information to the control center. Furthermore, as satellite-based marine networks, such as the Starlink program, are gradually implemented [22], the problem of data backhaul on all types of boats may be solved.

We quantify possible parameters influencing proximity detection results in this study and provide a solid reference base for future proximity detection algorithm development.

4. Impact of Quantization of Bluetooth RSSI Values

4.1. Statistical Analysis

Due to the limited space of the ship, most of the time, passengers are in the sitting pose instead of the standing pose. Therefore, it is necessary to study the influence on proximity detection in the case of two different poses, sitting and standing, in order to provide a basis for future research related to the theoretical method of distance identification.

Experimental data are obtained from the PACT consortium. RSSI values are reported by smartphones. These quantization bins are represented by all possible values reported by the RSSI of each smartphone [20]. The larger the quantization of RSS, the better RSS represents a Bluetooth signal. Bluetooth with more quantization steps should provide a better method for proximity detection [23]. If only the integer number is used for proximity detection, the chance of any two locations having exact locations would increase and degrade the performance of the proximity detection technique [24].

Typically, most of the research studies involving indoor positioning systems calculate the average values of RSSI and record them as real numbers [25]. This reduces the problem of the quantization effect in development [26]. A comparison of RSSI from the different distances and poses is shown in Table 1. The quantization impact can also be mitigated by using the mode and median. Table 1 shows how RSSI values of the mean, median, and mode change over time for the same distance. Each distance and pose collected 3240 RSSI samples over three minutes (18 samples/second) in order to calculate the summary statistics in the table.

Table 1. Statistics of RSSI measured from different distances (Sit and Stand cases) (source: PACT dataset).

Statistics	**3 ft**	**4 ft**	**5 ft**	**6 ft**	**8 ft**	**10 ft**	**12 ft**	**15 ft**
Mean (Sit)	−58.2	−62	−66.5	−69.5	−67.5	−68.0	−72.4	−71.2
Median (Sit)	−56	−61	−66	−68	−67	−68	−72	−71
Mode (Sit)	−51	−57	−62	−68	−61	−72	−72	−72
Standard Deviation (Sit)	6.1	6.7	5.9	7.6	6.5	7.4	6.7	4.9
Skewness (Sit)	−0.62	−0.62	−0.64	−1.03	−0.76	−0.14	−0.47	0.06
Range (Sit)	26	36	40	40	35	40	41	33
Minimum (Sit)	−76	−86	−93	−97	−91	−93	−98	−89
Maximum (Sit)	−50	−50	−53	−57	−56	−53	−57	−56
Statistics	**3 ft**	**4 ft**	**5 ft**	**6 ft**	**8 ft**	**10 ft**	**12 ft**	**15 ft**
Mean (Stand)	−54.0	−57.9	−58.0	−58.6	−60.7	−61.0	−67.4	−70.6
Median (Stand)	−54	−57	−58	−58	−60	−60	−66	−69
Mode (Stand)	−57	−54	−54	−55	−61	−56	−66	−65
Standard Deviation (Stand)	5.2	6.2	5.5	5.2	4.9	5.4	5.8	6.2
Skewness (Stand)	−0.18	−1.37	−1.36	−0.94	−0.67	−0.6	−0.8	−0.96
Range (Stand)	35	45	43	33	35	36	44	36
Minimum (Stand)	−77	−92	−92	−82	−85	−86	−97	−95
Maximum (Stand)	−42	−47	−49	−49	−50	−50	−53	−59

The means are different by about 0.6 dBm to 10.9 dBm in various poses at the same distance. Range, standard deviation, and skewness are also diverse. A particular point of interest is that the mean of RSSI (Sit and Stand) is the most similar at 15 ft. RSSI will rapidly deteriorate as the distance between two points increases. At 8 ft, the RSSI value becomes more vital in the sitting pose. Mean and median readings, −67.5 dBm and −67 dBm, are nearly identical. The mode value, however, is −61 dBm. The mode value at 6 ft and the mode value at 8 ft is 7 dBm. The mean and median readings are only 2.5 and 1 dBm, respectively. If proximity is calculated by using mode as a representative value of RSSI, the result may be around 4 ft; however, if proximity is calculated using mean and median, the result will be between 5 ft and 6 ft. To put it another way, using mode as an RSSI proxy for a sitting pose at an 8 ft will result in more significant inaccuracy. Mean and median values in the standing pose show a declining tendency with increasing distance. The 4 ft to 6 ft mode values are more significant than the 3 ft mode values. This contradicts the RSSI rule, which states that RSSI decreases with distance. The mode value at 4 ft distance is 7 dBm higher than at 3 ft, resulting in a substantial mistake in distance computation. Finally, we find that mean and median RSSI values are recommended for calculating proximity detection, whereas the mode value is not.

Standard deviation is a measure of a set of value variability or dispersion. A low standard deviation shows that these values tend to be close to the average value of the group, whereas a high standard deviation indicates that these values are spread across a broader range. As shown in Table 1, standard deviation is the lowest at 15 ft and largest at 6 ft for the sitting pose. However, the most significant distance error occurs at 8 ft. In standing poses, the median values are the same for 5 ft and 6 ft and 8 ft and 10 ft. That is to say that using the median value of RSSI for proximity detection will produce a significant error at these distances. In addition, it is not possible to reduce these errors from the standard deviation at these distances.

Considering only the dispersion of Bluetooth RSSI values from the mean value, whether in sitting or standing poses, does not minimize errors. In skewness, all distributions are left-skewed, except for the 15 ft RSSI distribution in sitting pose, which is right-skewed. In addition, the minimum and maximum values of RSSI also do not conform to the rule that RSSI decays with increasing distance.

From the above analysis, we conclude that the mean value of RSSI can be used to reduce error rather than relying on median, mode, minimum, and maximum when conducting proximity detection in two different poses: that of sitting and standing. If only RSSI dispersion is considered, reducing errors becomes challenging. Moreover, in most cases, RSSI values almost wholly belong to left-skewed distributions.

Traditionally, RSSI is believed to be log-normally distributed according to the large-scale fading model impact on receiver design and coverage. There is still a lack of necessary understanding of RSSI properties from the perspective of proximity detection [27].

Due to propagating effects, such as reflection, diffraction, and dispersion caused by dense multipath and indoor environments, it is challenging to predict radio frequency (RF) signal variations [28]. The multi-path fading effect results from a constructive or destructive combination of multiple signal copies at the receiver, causing the signal received to fluctuate in a particular area around the mean value [29]. In the case of large-scale decreases and small-scale declines, the received signal is generally modeled [30]. Note that the measurements average small-scale fading results when RSSI is average [31]. However, these results do not consider an in-depth analysis of RSSI distribution.

Observations from datasets of 3 ft (Sit and Stand) histograms indicated that the different distribution shapes of the RSSI occurred for varying poses. The reason is that the upper and lower bounds of measurable RSSI at each distance cause other forms of distributions.

Figures 4 and 5 illustrate slightly skewed RSSI distributions measured from 3 ft (Sit and Stand). Two samples of RSSI histograms were collected from 3 ft (Sit) and 3 ft (Stand) in Figures 4 and 5. This study compared the sitting pose with the standing posture for three minutes at 3 ft—the histogram of 3 ft (Sit) is shown in the left-skewed RSSI distribution in Figure 4. The histogram of 3 ft (Stand) is shown as an almost normal-skewed RSSI distribution in Figure 5. The authors of [32] report a normal distribution where the measurement in that study is taken inside an office room. However, the fact is that people's poses can influence the distribution of RSSI.

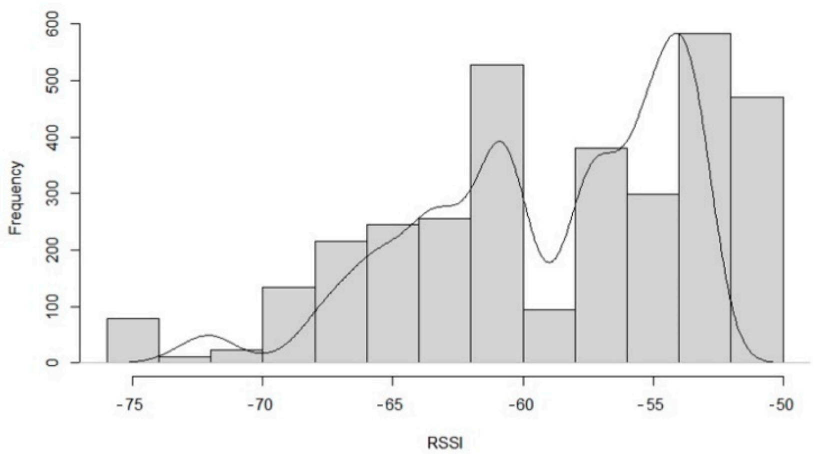

Figure 4. Samples of RSSI distribution over three minutes (3 ft, Sit).

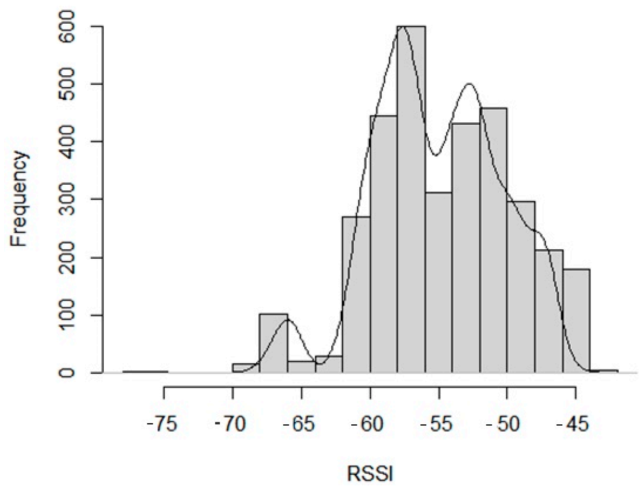

Figure 5. Samples of RSSI distribution over three minutes (3 ft, Stand).

The samples are predominantly concentrated between −65 dBm and −50 dBm in the sitting pose and between −60 dBm and −50 dBm in the standing pose. In other words, different poses slightly change the distribution of RSSI. RSSI distribution is closer to the normal distribution in the standing posture. In addition, it can be observed from Figures 4 and 5 that different postures cause different ranges of variation in RSSI, which can cause inconsistencies to occur in mean RSSI values of these two poses, which may form their respective characteristics. From the above analysis, we conclude that there is a combination of mean value and skewness characteristics of RSSI in different poses. In the case of close distance, the current posture of ship passengers can be identified based on the mean and skewness of RSSI.

4.2. Autocorrelation Analysis

Figure 6 shows the variation of RSSI for two different poses of 3 ft and 15 ft. The measurement is performed over a continuous period of 3 min on different distances and poses. The RSSI range difference of sitting and standing poses is evident at 3 ft. However, it is not distinct at 15 ft—the RSSI of sitting and standing at 15 ft stabilized in a similar range. The RSSI of sitting and standing postures is clearly distinguished at 3 ft. RSSI content is almost identical with different poses at 15 ft. The RSSI of stand poses fluctuates mainly between −50 dBm and −55 dBm in the range of 0 to 1000 in the horizontal coordinate of 3 ft. In that range, the RSSI fluctuation interval of the sitting poses is two: One is in the horizontal coordinate of 0 to 500 range where the RSSI fluctuation interval is −55 dBm to −70 dBm. The other is in the horizontal coordinate of the 500 to 1000 range; the RSSI fluctuation interval is −50 dBm to −55 dBm. That is to say that in a specific time range of a close distance case, there is a significant difference in RSSI for various poses, and in the long-distance case, this difference gradually decreases. From the above analysis, we conclude that as distance increases, the difference in RSSI at various poses gradually decreases. Mean and skewness features for distinguishing different poses gradually disappear. In the case of close distance, the RSSI of different poses have various fluctuation intervals in different periods.

This study performs autocorrelation analysis in order to determine how correlated RSSI values are over time. The equation for autocorrelation is as follows.

$$R(k) = \frac{1}{(n-k)\sigma^2} \sum_{t=1}^{n-k} (x_t - \mu)(x_{t+k} - \mu) \quad (1)$$

Exploring the autocorrelation of RSSI focuses on measuring the relationship between RSSI at the current moment and the next moment. However, the relationship between the individual and RSSI also needs to be considered. Therefore, variance and mean are also included in the calculation. σ is variance, and μ is mean. x_t is the RSSI at time t, and x_{t+k} is the RSSI at time $t + k$.

This study assumes that RSSI is time-dependent. The correlograms are plotted in Figure 7. Figure 7 depicts similar shapes for 3 ft and 15 ft in sitting and standing pose. Note that the 15 ft (Sit and Stand) plot in Figure 7 has much smaller correlation coefficients at more considerable time lags, which indicated that dependences of RSSI sample reduced faster in 15 ft. This implies a faster signal change resulting from rapid change in the distance.

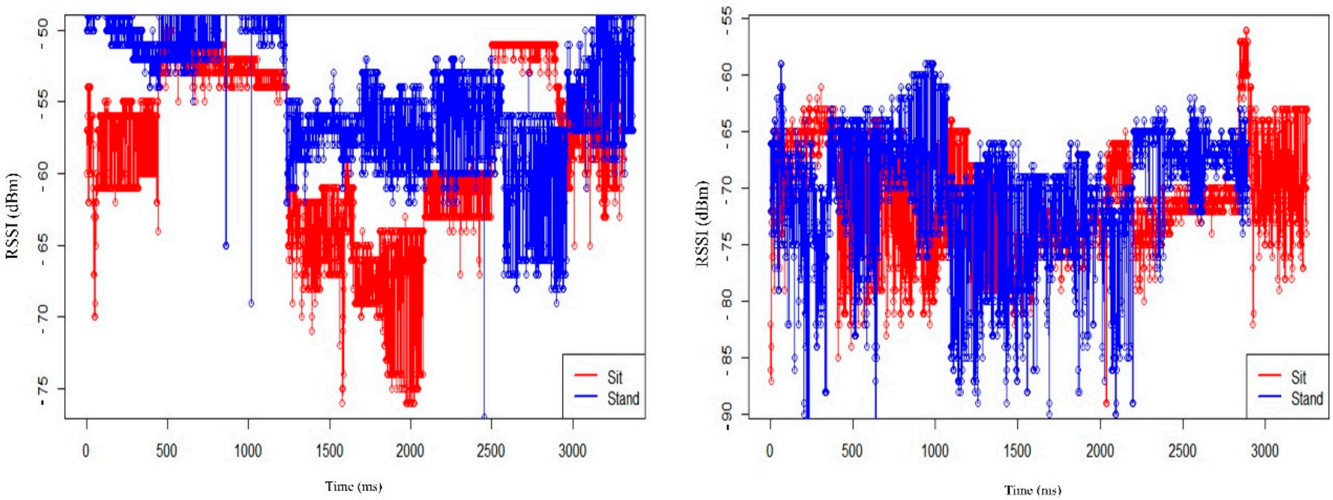

3 ft **15 ft**

Figure 6. RSSI over 3 min at 3 ft and 15 ft (Sit, Stand).

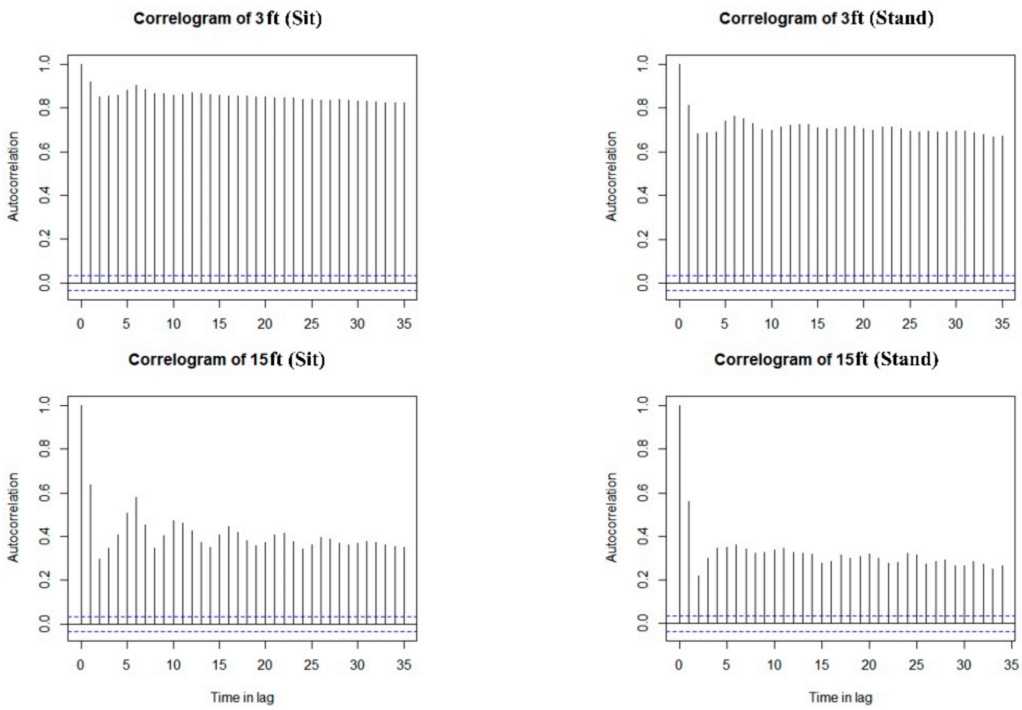

Figure 7. Correlograms of RSSI (3 ft and 15 ft, Sit and Stand).

Meanwhile, the RSSI of the standing pose correlation coefficients at the same distance had smaller values than the sitting pose. The visual tests for this sample suggest the possibility of a stationary process. The higher the distance, the larger the autocorrelation coefficient, and the smaller the distance, the smaller the autocorrelation coefficient, according to the correlogram. The influence of different postures on the autocorrelation coefficient is relatively minimal from the standpoint of the posture. The autocorrelation coefficient of the standing posture is slightly lower than that of the sitting posture. In other words, regardless of whether you sit or stand, the RSSI autocorrelation coefficient does not change appreciably. Note that since autocorrelations in the plots are significantly non-zero, the RSSI does have a strong correlation between consecutive samples as an assumption.

4.3. Visualize RSSI Patterns in Different Poses

Figure 8 shows two-dimensional plots of RSSI patterns from different poses at the same distance. The x-axis represents the RSSI of the sitting posture. The y-axis represents the RSSI of the standing posture. Note that the pattern of RSSIs of different poses cannot be grouped into clusters. The degree of separation does not increase as distance changes from 3 ft to 15 ft at different poses. This observation suggests that signals with more significant standard deviations (or variance) will make it more challenging to perform proximity detection. The 3-feet distance, as shown in Figure 9, has a substantially more distinct patterns than the other lengths. As a result, RSSI data from sitting and standing poses may be combined to obtain a 3-feet distance marker. On the other hand, the different distances produce no discernible pattern change. The RSSs of the sitting and standing poses for the 3-feet distance is closer simultaneously, but the RSSs of the two poses for the other ranges are further away.

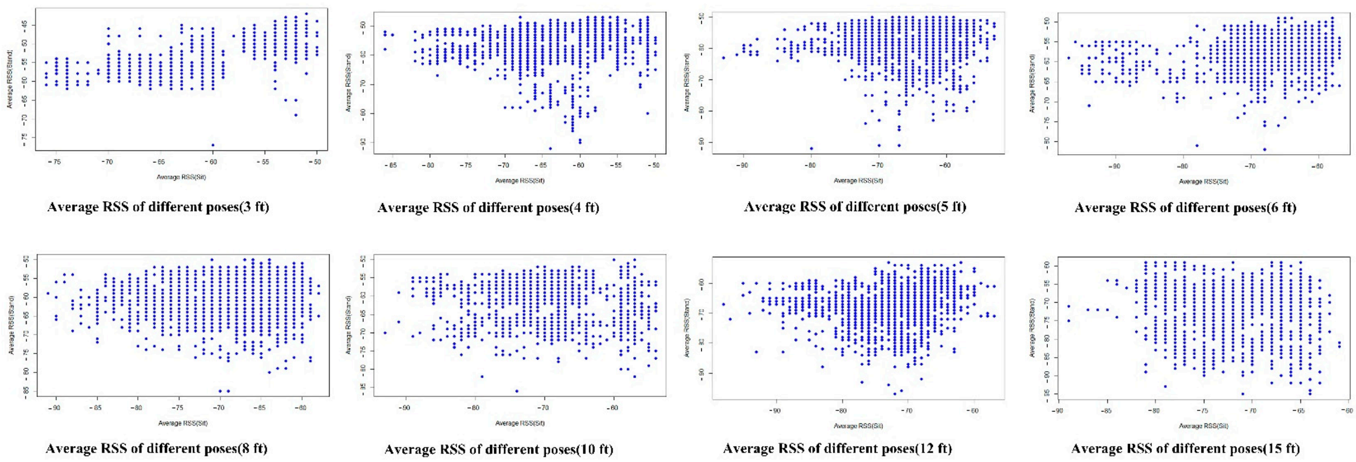

Figure 8. RSSI of different poses and distances.

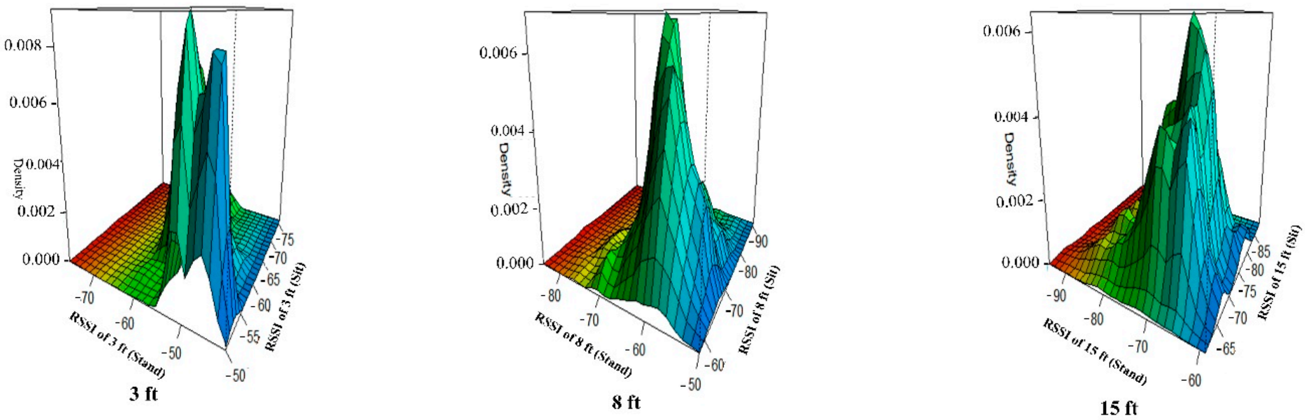

Figure 9. Three-dimensional density plots of RSSI with 3 ft, 8 ft, and 15 ft.

The overlap between the patterns becomes a bigger problem for proximity detection as the number of distances increases. This can be depicted in Figure 9 when plotting the three dimensions for RSSI patterns. The density of the y-axis is the kernel density estimation (KDE) [33]. KDE is a non-parametric method used for estimating a random variable probability density function. The RSSI value can be considered as a point. The density of issues can be calculated to reveal the degree of clustering points. This degree of aggregation can form a pattern. Under different conditions, different degrees of the collection show different designs. KDE can visualize RSSI patterns. The formula is as follows:

$$f_h(x) = \frac{1}{nh} \sum_{i=1}^{n} K\left(\frac{x - x_i}{h}\right) \tag{2}$$

where K is the kernel (a non-negative function), and h is the bandwidth's smoothing parameter ($h > 0$). x is any given RSSI. n is the number of RSSI. Figure 9 shows that the two RSSI patterns are easier to classify at 3 ft. However, the overlap between the patterns occurs at 8 ft and 15 ft. In general, the increasing number of RSSI data is one method of separating different distances. The effect of peoples' poses on the RSSI signal gradually decreases with distance [34]. Note that it is difficult to illustrate the frequency of each pattern at 3 ft, but we may deduce that the highest frequency of occurrence will be at the center of each cluster. In the case of long distances, the effect of the different poses of people producing different patterns of RSSI becomes smaller. In real situations, this intermittence of received signals can result in incomplete or censored RSSI patterns during the proximity detection phase [35]. This affects proximity detection performance when matching a preliminary RSSI pattern to proximity detection.

In general, RSSI distance calculation is performed with a log-distance path loss model. However, only one RSSI value can be entered into this model. A single RSSI value is usually a representative RSSI value over time. This can be mean, median, mode, minimum, and maximum, and it can be different for the same distance due to the effects of the pose on RSSI distribution. This can cause a mistake in distance calculation. This mistake can reduce the accuracy of trilateral localization. Fingerprint profiles are also produced by using representative RSSI values, resulting in errors when comparing fingerprint profiles.

While the pose impacts the RSSI distribution, this impact is constant over time. While the RSSI distribution for each position is different for the same distance, this difference can be used as a feature. In other words, RSSI can be marked in advance by pose and distance. For each posture and distance, the RSSI distribution is calculated. The RSSI distribution is collected from the user's device during user positioning phases, and it is calculated. The most similar distribution is then compared in order to reduce errors caused by the pose's effect on RSSI. The basic principle is identical to a fingerprint map, except that the RSSI data are replaced with distribution data.

5. Conclusions

The shut-off spatial environment of ships facilitates the spread of viruses. The most critical aspect of pandemic preparation is the timely detection of close contacts on board. Proximity detection of smartphones can identify close contacts. Essential data for proximity detection include the Bluetooth RSSI signal. In this paper, a statistical analysis compares publicly available Bluetooth RSSI signal data in sitting and standing poses.

The proximity detection error is lower than in medium, mode, minimum and maximum with the mean RSSI value. If only RSSI dispersion is considered, reducing the error is difficult to achieve. The RSSI values in the majority of cases are almost all left-skewed. The mean and skewness of RSSI are combined with other features. The current pose, either sitting or standing, of the person on board can be determined based on the mean and skewness of RSSI in the event of a close distance.

The difference of RSSI in different poses decreases as distance increases. The feature of mean and skewness gradually disappears for longer distances. RSSIs of the two poses in various periods have different but closer fluctuation intervals. These characteristics enhance the precise detection of proximity and, under certain conditions, determine the ship passenger's pose. In order to prevent the further spread of COVID-19 between ship passengers, this method can be used to precisely identify close contacts with high-precision proximity detection.

Author Contributions: Conceptualization, Q.L.; methodology, Q.L.; software, Q.L.; validation, Q.L.; formal analysis, Q.L.; investigation, Q.L.; resources, Q.L.; data curation, Q.L.; writing—original draft preparation, Q.L.; writing—review and editing, J.S.; visualization, Q.L.; supervision, J.S.; project administration, J.S.; funding acquisition, J.S. All authors have read and agreed to the published version of the manuscript.

Funding: This research was supported by the Basic Science Research Program through the National Research Foundation of Korea (NRF) funded by the Ministry of Education (grant number: 2021R1I1A3056125).

Institutional Review Board Statement: Not applicable.

Informed Consent Statement: Not applicable.

Data Availability Statement: Not applicable.

Conflicts of Interest: The authors declare no conflict of interest.

References

1. Klein, N. International law perspectives on cruise ships and COVID-19. *J. Int. Humanit. Leg. Stud.* **2020**, *11*, 282–294. [CrossRef]
2. Batista, B.; Dickenson, D.; Gurski, K.; Kebe, M.; Rankin, N. Minimizing disease spread on a quarantined cruise ship: A model of COVID-19 with asymptomatic infections. *Math. Biosci.* **2020**, *329*, 108442. [CrossRef] [PubMed]
3. Fanoy, E.; Ummels, A.E.; Schokkenbroek, V.; Van Dijk, B.; Wiegmans, S.; Veenstra, T.; Van Der Eijk, A.; Sikkema, R.; De Raad, A. Outbreak of COVID-19 on an industrial ship. *Int. Marit. Health* **2021**, *72*, 87–92. [CrossRef] [PubMed]
4. Von Münster, T.; Kleine-Kampmann, S.; Hewelt, E.; Boldt, M.; Schlaich, C.; Strölin, P.; Oldenburg, M.; Dirksen-Fischer, M.; Harth, V. When the ship comes in–COVID-19 Ausbrüche an Bord von Frachtschiffen im Hamburger Hafen. *Flugmed. Trop. Reisemedizin-FTR* **2021**, *28*, 13–24. [CrossRef]
5. Plucinski, M.M.; Wallace, M.; Uehara, A.; Kurbatova, E.V.; Tobolowsky, F.A.; Schneider, Z.D.; Ishizumi, A.; Bozio, C.H. Coronavirus disease 2019 (COVID-19) in Americans aboard the Diamond Princess cruise ship. *Clin. Infect. Dis.* **2021**, *72*, 448–457. [CrossRef]
6. Azimi, P.; Keshavarz, Z.; Laurent, J.G.C. Mechanistic transmission modeling of COVID-19 on the Diamond Princess cruise ship demonstrates the importance of aerosol transmission. *Proc. Natl. Acad. Sci. USA* **2021**, *118*, e2015482118. [CrossRef]
7. Battineni, G.; Sagaro, G.G.; Chintalapudi, N.; Di Canio, M. Assessment of awareness and knowledge on novel coronavirus (COVID-19) pandemic among seafarers. *Healthcare* **2021**, *9*, 120. [CrossRef]
8. Chen, C.M.; Jyan, H.W.; Chien, S.C.; Jen, H.H. Containing COVID-19 among 627,386 persons in contact with the Diamond Princess cruise ship passengers who disembarked in Taiwan: Big data analytics. *J. Med. Internet Res.* **2020**, *22*, e19540. [CrossRef]
9. Hatke, G.F.; Montanari, M.; Appadwedula, S.; Wentz, M. Using Bluetooth Low Energy (BLE) signal strength estimation to facilitate contact tracing for COVID-19. *arXiv* **2020**, arXiv:2006.15711.
10. Meklenburg, J.; Specter, M.; Wentz, M.; Balakrishnan, H.; Chandrakasan, A.; Cohn, J. An Ultrasonic Ranging Method for the Private Automated Contact Tracing (PACT) Protocol. *arXiv* **2012**, arXiv:2012.04770.
11. Londner, T.; Saunders, J.; Schuldt, D.W.; Streilein, B. Simulated Automatic Exposure Notification (SimAEN): Exploring the Effects of Interventions on the Spread of COVID. *Priv. Autom. Contact Tracing* **2020**, *1*, 1–23.
12. Alekseyev, J.; Dixon, E.; Woltz, V.L.A.; Weitzner, D. Realizing the Promise of Automated Exposure Notification (AEN) Technology to Control the Spread of COVID-19: Recommendations for Smartphone App Deployment, Use, and Iterative Assessmen. *arXiv* **2020**, arXiv:2012.09232.
13. Mariscotti, A. Experimental determination of the propagation of wireless signals on board a cruise ship. *Measurement* **2011**, *44*, 743–749. [CrossRef]
14. Zhou, C.; Yuan, J.; Liu, H.; Qiu, J. Bluetooth indoor positioning based on RSSI and Kalman filter. *Wirel. Pers. Commun.* **2017**, *96*, 4115–4130. [CrossRef]
15. Namie, H.; Suzuki, O. Indoor Location Estimation by Bluetooth Low Energy for Pedestrian Navigation. *IEEJ J. Ind. Appl.* **2020**, *1*, 20003604. [CrossRef]
16. Kaemarungsi, K.; Krishnamurthy, P. Properties of indoor received signal strength for WLAN location fingerprinting. In Proceedings of the First Annual International Conference on Mobile and Ubiquitous Systems: Networking and Services, Boston, MA, USA, 22–26 August 2004.
17. Using Machine Learning to Perform Proximity Detection-Classifying Bluetooth Beacon RSSI Values. Available online: https://www.preprints.org/manuscript/202009.0508/v1 (accessed on 12 November 2020).
18. Madani, B.; Alagi, H.; Hein, B.; Arntzen, A.A. Machine Learning for Capacitive Proximity Sensor Data. In Proceedings of the SDPS 22nd International Conference on Emerging Trends and Technologies in Convergence Solutions, Birmingham, AL, USA, 5–9 November 2017.

19. Su, Z.; Pahlavan, K.; Agu, E. Performance Evaluation of COVID-19 Proximity Detection Using Bluetooth LE Signal. *IEEE Access* **2021**, *9*, 38891–38906. [CrossRef] [PubMed]
20. Rivest, R.L.; Callas, J.; Canetti, R.; Esvelt, K.; Gillmor, D.K.; Kalai, Y.T. *The PACT Protocol Specification*; Private Automated Contact Tracing Team: Cambridge, MA, USA, 2020.
21. Son, J.; Lin, Q. *Precision location tracking and data mining on IoT-based ships for safety and public hygiene of large ship occupants, In the report of Science & Technology Planning Project*; Busan Innovation Institute of Industry: Busan, Korea, 2020; pp. 1–86.
22. Del Portillo, I.; Cameron, B.G.; Crawley, E.F. A technical comparison of three low earth orbit satellite constellation systems to provide global broadband. *Acta Astronaut.* **2019**, *159*, 123–135. [CrossRef]
23. Lovett, T.; Briers, M.; Charalambides, M.; Jersakova, R.; Lomax, J.; Holmes, C. Inferring proximity from bluetooth low energy rssi with unscented Kalman smoothers. *arXiv* **2020**, arXiv:2007.05057.
24. Sheikh, M.U.; Badihi, B.; Ruttik, K.; Jäntti, R. Adaptive Physical Layer Selection for Bluetooth 5: Measurements and Simulations. *Wirel. Commun. Mob. Comput.* **2021**, *2021*, 8842919. [CrossRef]
25. Liu, S.; Jiang, Y.; Striegel, A. Face-to-face proximity estimationusing bluetooth on smartphones. *IEEE Trans. Mob. Comput.* **2013**, *13*, 811–823. [CrossRef]
26. Naghdi, S.; O'Keefe, K. Trilateration with BLE RSSI accounting for pathloss due to human obstacles. In Proceedings of the 2019 International Conference on Indoor Positioning and Indoor Navigation (IPIN), Pisa, Italy, 30 September–3 October 2019.
27. Park, S.; Choi, Y. Bluetooth Beacon-Based Mine Production Management Application to Support Ore Haulage Operations in Underground Mines. *Sustainability* **2021**, *13*, 2281. [CrossRef]
28. Sansano-Sansano, E.; Aranda, F.J.; Montoliu, R.; Álvarez, F.J. BLE-GSpeed: A new BLE-based dataset to estimate user gait speed. *Data* **2020**, *5*, 115. [CrossRef]
29. Cominelli, M.; Patras, P.; Gringoli, F. Dead on arrival: An empirical study of the Bluetooth 5.1 positioning system. In Proceedings of the 13th International Workshop on Wireless Network Testbeds, Los Cabos, Mexico, 25 October 2019.
30. Suryavanshi, N.B.; Reddy, K.V.; Chandrika, V.R. Direction finding capability in Bluetooth 5.1 standard. In Proceedings of the International Conference on Ubiquitous Communications and Network Computing, Bangalore, India, 8–10 February 2019.
31. Lymberopoulos, D.; Liu, J.; Yang, X. A realistic evaluation and comparison of indoor location technologies: Experiences and lessons learned. In Proceedings of the 14th International Conference on Information Processing in Sensor Networks, Seattle, WA, USA, 13–16 April 2015.
32. Faragher, R.; Harle, R. An analysis of the accuracy of Bluetooth low energy for indoor positioning applications. In Proceedings of the 27th International Technical Meeting of the Satellite Division of the Institute of Navigation, Tampa, FL, USA, 8–12 September 2014.
33. Kuk, G. Strategic interaction and knowledge sharing in the KDE developer mailing list. *Manag. Sci.* **2006**, *52*, 1031–1042. [CrossRef]
34. Guo, Y.; Zheng, J.; Zhu, W. iBeacon Indoor Positioning Method Combined with Real-Time Anomaly Rate to Determine Weight Matrix. *Sensors* **2021**, *21*, 120. [CrossRef] [PubMed]
35. Liu, L.; Li, B.; Yang, L. Real-time indoor positioning approach using iBeacons and smartphone sensors. *Appl. Sci.* **2020**, *10*, 2003. [CrossRef]